

See discussions, stats, and author profiles for this publication at: <https://www.researchgate.net/publication/231403300>

Temperature dependence of the rate constants for the reactions of ethynyl radical with acetylene, hydrogen, and deuterium

ARTICLE *in* THE JOURNAL OF PHYSICAL CHEMISTRY · NOVEMBER 1992

Impact Factor: 2.78 · DOI: 10.1021/j100203a048

CITATIONS

27

READS

10

4 AUTHORS, INCLUDING:



Mitsuo Koshi

The University of Tokyo

168 PUBLICATIONS 1,768 CITATIONS

SEE PROFILE

- (2) (a) Douglas, A. E. *Discuss. Faraday Soc.* **1963**, 35, 158. (b) Walsh, A. D.; Warsop, P. A. *Trans. Faraday Soc.* **1961**, 57, 345. (c) Ziegler, L. D.; Hudson, B. J. *J. Phys. Chem.* **1984**, 88, 1110. (d) Vaida, V.; Hess, W.; Roebber, J. L. *J. Phys. Chem.* **1984**, 88, 3397.
- (3) Halpern, A. M.; Ondrechen, M. J.; Ziegler, L. D. *J. Am. Chem. Soc.* **1986**, 108, 3907.
- (4) Halpern, A. M. *Mol. Photochem.* **1973**, 5, 517.
- (5) Meyerhoffer, A.; Carlstrom, D. *Acta Crystallogr., Sect. B* **1969**, 25, 1119.
- (6) (a) Halpern, A. M.; Roebber, J. L.; Weiss, K. *J. Chem. Phys.* **1968**, 49, 1348. (b) Halpern, A. M. *J. Am. Chem. Soc.* **1974**, 96, 7655.
- (7) Halpern, A. M. *J. Am. Chem. Soc.* **1974**, 96, 4392.
- (8) Halpern, A. M.; Ravinet, P.; Sternfels, R. J. *J. Am. Chem. Soc.* **1977**, 99, 169.
- (9) Ruggles, C. J.; Halpern, A. M. *J. Am. Chem. Soc.* **1988**, 110, 5692.
- (10) Bock, H.; Goebel, I.; Zdenek, H.; Liedle, S.; Oberhammer, H. *Angew. Chem., Int. Ed. Engl.* **1991**, 30, 187.
- (11) (a) Leonard, N. J.; Coll, J. C.; Wang, A. H.-J.; Missavage, R. J.; Paul, I. C. *J. Am. Chem. Soc.* **1971**, 93, 4628. (b) Wang, A. H.-J.; Missavage, R. J.; Byrn, S. R.; Paul, I. C. *J. Am. Chem. Soc.* **1972**, 94, 7100.
- (12) Halpern, A. M.; Gartman, T. *J. Am. Chem. Soc.* **1974**, 96, 1393.
- (13) Halpern, A. M.; Wong, D. K. *Chem. Phys. Lett.* **1976**, 37, 416.
- (14) Halpern, A. M.; Frye, S. L. *J. Phys. Chem.* **1988**, 92, 6620.
- (15) Frye, S. L.; Ko, J.; Halpern, A. M. *Photochem. Photobiol.* **1984**, 40, 555.
- (16) MOPAC, Version 6.0, QCPE 455, Quantum Chemistry Program Exchange, Indiana University, Bloomington, IN 47405.
- (17) Frisch, M. J.; Head-Gordon, M.; Trucks, G. W.; Foresman, J. B.; Schlegel, H. B.; Raghavachari, K.; Robb, M. A.; Binkley, J. S.; Gonzalez, C.; Defrees, D. J.; Fox, D. J.; Whiteside, R. A.; Seeger, R.; Melius, C. F.; Baker, J.; Martin, R. L.; Kahn, L. R.; Stewart, J. J. P.; Topiol, S.; Pople, J. A.; *Gaussian 90*, Rev. I; Gaussian, Inc.: Pittsburgh, PA, 1990.
- (18) Swalen, J. D.; Ibers, J. A. *J. Chem. Phys.* **1962**, 36, 1914.
- (19) Eades, R. A.; Weil, D. A.; Dixon, D. A.; Douglass, C. H., Jr. *J. Chem. Phys.* **1981**, 85, 976.
- (20) Chin, S. KGNRA, Version 4.0, IBM Corp., Kingston, NY 12401, 1991.
- (21) Aue, D. H.; Webb, H. M.; Bowers, M. T. *J. Am. Chem. Soc.* **1975**, 97, 4136.
- (22) Reference 6: Robin, M. B. *Higher Excited States of Polyatomic Molecules*; Academic Press: New York, 1974; Vol. 1, pp 8-47.
- (23) (a) Matsumi, Y.; Obi, K. *Chem. Phys.* **1980**, 49, 87. (b) Cureton, C. G.; Hara, K.; O'Connor, D. V.; Phillips, D. *Chem. Phys.* **1981**, 63, 31. (c) Asscher, M.; Haas, Y. *Appl. Phys.* **1982**, 76, 291.
- (24) Birks, J. B. *Photophysics of Aromatic Molecules*; Wiley-Interscience: London, 1970; p 51.
- (25) Reference 24, p 88, eq 4.20.
- (26) See Halpern, A. M. In *The Chemistry of Functional Groups*; Patai, S., Ed.; Wiley & Sons: Chichester, 1982; Supplement F, Part 2, Chapter 5, pp 155-180.
- (27) (a) Reference 12. (b) Halpern, A. M. *J. Am. Chem. Soc.* **1974**, 96, 4392. (c) Halpern, A. M.; Chan, P. P. *J. Am. Chem. Soc.* **1974**, 97, 2971. (d) Nosowitz, M.; Halpern, A. M. *J. Phys. Chem.* **1986**, 90, 906.
- (28) Halpern, A. M.; Wryzykowska, K. *J. Photochem.* **1981**, 15, 147.
- (29) Halpern, A. M. *J. Phys. Chem.* **1981**, 85, 1682.
- (30) Halpern, A. M.; Weiss, K. *J. Am. Chem. Soc.* **1968**, 90, 6297.
- (31) Reference 6b.
- (32) Halpern, A. M.; Ruggles, C. J.; Ames, A. *J. Phys. Chem.* **1989**, 93, 3448.
- (33) Nelson, R. D., Jr.; Lide, D. R., Jr.; Maryott, A. A. Selected Values of Electric Dipole Moments of Molecules in the Gas Phase. *Natl. Stand. Ref. Data Ser.* **1967**, 10, 13-26.
- (34) Wolrab, J. E.; Laurie, V. W. *J. Chem. Phys.* **1969**, 51, 1580.

Temperature Dependence of the Rate Constants for the Reactions of C₂H with C₂H₂, H₂, and D₂

Mitsuo Koshi,* Koichi Fukuda, Kenshu Kamiya,[†] and Hiroyuki Matsui

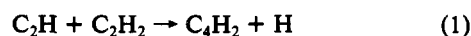
Department of Reaction Chemistry, The University of Tokyo, 7-3-1 Hongo, Bunkyo-ku, Tokyo 113, Japan

(Received: June 5, 1992)

Reactions of the ethynyl (C₂H) radical with C₂H₂, H₂, and D₂ were studied over the temperature range 298-438 K by time-resolved mass spectrometry. The rate of the reaction with C₂H₂ was followed by measuring the appearance rate of C₄H₂. The rates of the reactions with H₂ and D₂ were deduced by measuring the dependence of C₄H₂ production (arising from the reaction of C₂H with the C₂H₂ precursor) on the partial pressure of added H₂ or D₂. The rate constants for the reaction C₂H + C₂H₂ → C₄H₂ + H were also measured following reflected shock waves by monitoring H atom resonant absorption at 121.6 nm. In both experiments, the C₂H radical was generated by ArF (193-nm) laser photolysis of C₂H₂. A rate constant of $(1.5 \pm 0.3) \times 10^{-10} \text{ cm}^3 \text{ molecule}^{-1} \text{ s}^{-1}$ was obtained for reaction 1 without any temperature dependence at $T = 298\text{--}2177 \text{ K}$. The results for the reactions C₂H + H₂ → C₂H₂ + H and C₂H + D₂ → C₂HD + D could be represented by the Arrhenius expressions, $k_2 = (1.8 \pm 1.0) \times 10^{-11} \exp(-1090 \pm 299)/T$ and $k_3 = (1.4 \pm 0.8) \times 10^{-11} \exp(-1377 \pm 301)/T \text{ cm}^3 \text{ molecule}^{-1} \text{ s}^{-1}$, over the range of $T = 298\text{--}438 \text{ K}$. The classical barrier height for reactions 2 and 3 was estimated to be 2 kcal/mol on the basis of conventional transition-state theory. The isotope effects on reactions 2 and 3 calculated with Wigner tunneling correction were in good agreement with the present results.

1. Introduction

The ethynyl radical, C₂H, is known to be important as a precursor for soot formation¹ in the pyrolysis of C₂H₂, and the rate constants for the C₂H reactions with C₂H₂ and H₂,



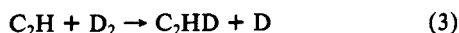
have been measured at room temperature by several groups.²⁻⁹ Laufer and Bass² determined the rate constants of reactions 1 and 2 by observing the appearance rate of C₄H₂ in the flash photolysis of C₂H₂. On the other hand, Stephens et al.⁷ determined the rate constants by following the time decay of a C₂H infrared transient absorption line using color center laser spectroscopy. Their values of k_1 and k_2 are about 5 and 3 times larger than those of Laufer

and Bass. In order to explain this discrepancy, Stephens et al. argued the formation of a long-lived intermediate (such as C₄H₃ in reaction 1 and C₂H₃ in reaction 2). However, the value of k_1 derived by Stephens et al. is in good agreement with the recent values of Shin and Michael⁸ and of Koshi et al.⁹ In our previous work,⁹ the rate constants of reactions 1 and 2 were derived from the production rates of H atoms by using a LIF technique at the Lyman α wavelength. The production rates of C₄H₂ were also followed by using mass spectrometry. The rate constants obtained from the production rates of H atoms and of C₄H₂ agreed with each other within the experimental errors. It was also found that all the C₂H radicals initially formed by the photolysis of C₂H₂ were converted to H atoms by reactions 1 and 2. Therefore, it is concluded that reactions 1 and 2 proceed without forming the long-lived intermediates, and their rate constants at room temperature are now well established.

In spite of these studies at room temperature, very few measurements of the temperature-dependent rate constants have been

[†] Present address: School of Pharmaceutical Science, Kitasato University, 5-9-1 Shirokane, Minato-ku Tokyo 108, Japan.

reported to date for these reactions. The temperature dependence of the rate constant of reaction 2 is of interest for the modeling of soot formation in hydrocarbon combustion. Also, measurement of the temperature dependence of the isotope ratio for the $C_2H + H_2/D_2$ reactions is important to obtain information on the structure of the transition state and to examine the effect of tunneling on the rate constant.⁹ In the present study, the rate constants for reactions 1–3 were determined by using the laser-



photolysis/time-resolved mass spectrometry (LP/MS) technique over the temperature range of $T = 298$ – 438 K. The resulting isotope ratio of k_2/k_3 was compared with conventional transition-state theory combined with the ab initio calculation of the transition state.

The rate constant of reaction 1 at much higher temperatures ($T = 1000$ – 2200 K) has been measured by Shin and Micheal⁸ using the laser-photolysis/shock-tube (LP/ST) technique. We have also applied the LP/ST technique to determine the rate constants of reactions 1 and 2.¹⁰ Since our high-temperature rate constant of reaction 1 was smaller than that of Shin and Micheal, we re-examined this rate constant, and a new value is presented here.

2. Experimental Section

The apparatus used in the LP/MS experiments is identical to that used in the kinetic studies previously.^{9,11,12} A Pyrex flow cell of 1.6-cm inner diameter was installed in the vacuum chamber of a quadrupole mass spectrometer. It was found that rate measurements were significantly affected by a heterogeneous loss process which was kinetically first order. A coating on the wall of the Pyrex cell with Teflon film was essential to prevent this heterogeneous loss. The rate of loss without coating was measured to be 600 s^{-1} , whereas it was reduced to less than 100 s^{-1} with Teflon coating. Our preliminary report¹³ on the rate constants of the C_2H reactions measured with a reaction cell without Teflon coating might be less accurate because of the very fast loss rate of C_2H on the cell wall.

In the present experiments, the temperature of the cell was controlled with an electric heater in the range of $T = 298$ – 438 K. Gases in the cell were sampled continuously through a small orifice ($100\text{ }\mu\text{m}$) into the electron-impact ionization chamber of the mass spectrometer. A secondary electron multiplier, operated with pulse-counting mode, was used to detect the ion signals. The time profiles of the mass-selected signals were obtained by scanning the gate delay of the pulse counter with a fixed gate width of 50 or $100\text{ }\mu\text{s}$.

The C_2H radical was generated by ArF laser photolysis of C_2H_2 . The sample gas mixture (0.1 – 0.3 mTorr of C_2H_2 , 0 – 0.3 Torr of H_2 , or 0 – 0.7 Torr of D_2 at a total pressure of 5 Torr in He) was irradiated by an unfocused output of the ArF laser (Questek 2220) with typical fluence of 25 mJ/cm^2 . Since the yield of H atom production (and hence C_2H production) by 193-nm photolysis of C_2H_2 with this laser fluence has been estimated to be less than $[H]/[C_2H_2] = 2 \times 10^{-3}$ by using a vacuum UV-LIF technique,⁹ pseudo-first-order conditions (C_2H_2 or H_2 or D_2 in large excess) were always maintained in the present experiments. The C_4H_2 molecule was detected with an ionizer electron energy of 16 eV . Although experiments were conducted to detect the possible reaction products, e.g., C_3H_4 or C_3H_3 , none was detected except C_4H_2 . An attempt to detect C_2H also failed because of the large background ion signal from a fragment of C_2H_2 even with the low ionizer electron energy.

The LP/ST experiments were performed with a diaphragmless shock tube of 5-cm diameter. The details of the apparatus were described in our previous publications.^{14,15} Briefly, the sample gas mixture (20 – 100 ppm C_2H_2 , diluted in Ar) in reflected shock waves was irradiated with an unfocused output of an ArF excimer laser (Questek 2220) with a typical laser fluence of 67 mJ/cm^2 . The laser was triggered with a $50\text{-}\mu\text{s}$ delay time after the reflected shock wave passes through the observation section. The time-dependent concentration of the H atoms produced by the laser

TABLE I: Summary of the Rate Constants for the $C_2H + C_2H_2$ Reaction

T/K	$k_1/10^{-10}\text{ cm}^3\text{ molecule}^{-1}\text{ s}^{-1}$	T/K	$k_1/10^{-10}\text{ cm}^3\text{ molecule}^{-1}\text{ s}^{-1}$
298	1.4 ± 0.3^a	1613	1.8 ± 0.4
409	1.4 ± 0.7	1638	1.5 ± 0.8
438	1.3 ± 0.4	2010	1.5 ± 0.4
1600	1.5 ± 0.4	2177	1.9 ± 0.4

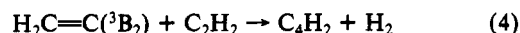
^a The errors are given to 2 standard deviations.

photolysis of C_2H_2 was monitored by using ARAS (atomic resonant absorption spectroscopy). The Lyman α resonant radiation at 121.6 nm from a microwave-excited discharge lamp (1% H_2 in He) was isolated by a 20-cm vacuum UV monochromator and was detected by a solar-blind photomultiplier (Hamamatsu R972). Absolute concentrations of H atoms were determined by using a calibration curve that was obtained from measurements of the steady-state concentrations of the H atom in the thermal decomposition of $H_2/N_2O/Ar$ mixtures.

C_2H_2 (99.8%), H_2 (99.995%), He (99.9995%), and Ar (99.9995%) were obtained from Nihon-Sanso and were used as delivered.

3. Results and Discussion

In the present LP/MS and LP/ST experiments, initial equal amounts of H atoms and C_2H radicals were produced by the ArF laser photolysis. The photochemical primary process in C_2H_2 is known to be fairly complex,^{5,8,16–20} and many radicals such as CH , C_2 , $C_2H(A^2\Pi)$, and triplet (3B_2) vinylidene have been observed. Possible complicating effects of these radicals on the kinetic measurements of the C_2H reactions were already discussed by Shin and Michael⁸ and Laufer et al.^{2,21,22} Satyapal and Bersohn²³ showed that the yields of H atoms by the ArF laser photolysis of C_2H_2 were proportional to the laser fluence up to 100 mJ/cm^2 . In the present LP/MS experiments, the laser fluence was kept low enough to prevent the production of CH or C_2 radicals by multiphoton processes.^{5,8} The total pressures and the concentrations of C_2H_2 were chosen so that the time scale for the rate measurements was much longer than the collisional deactivation rates of $C_2H(A^2\Pi)$.⁵ The collisional quenching rate of the triplet vinylidene radicals²⁴ could be slow under the present experimental conditions. Its successive reaction with C_2H_2 ,



could affect the production rate of C_4H_2 . However, the rate of this reaction ($k_4 = 5 \times 10^{-13}\text{ cm}^3\text{ molecule}^{-1}\text{ s}^{-1}$)¹⁶ is too slow to affect the observed production rates of C_4H_2 . This is further confirmed by the fact that the rate of H atom production and the rate of C_4H_2 production in the photolysis of C_2H_2 agreed well with each other and that the amount of H atoms produced by reaction 1 was balanced to the initial amount of C_2H .⁹ In addition, the rates of H atoms and C_4H_2 production were independent of the photolysis laser power. Therefore, the vinylidene radicals with long lifetimes cannot affect the time profiles of the H atoms and C_4H_2 . The H atom abstraction reaction, $H + C_2H_2 \rightarrow H_2 + C_2H$, is also slow under the present conditions.²⁴ Thus, the observed time profiles of C_4H_2 should exclusively reflect the reactions of the thermalized ground-state C_2H radical.

3.1. Reaction with C_2H_2 . An insert in Figure 1 shows a typical ion signal of C_4H_2 at $m/z = 50$ observed in the LP/MS experiments. The C_4H_2 signals were found to exhibit single-exponential rises. The first-order rise rates derived by a nonlinear least-squares fit to a single-exponential function are plotted in Figure 1 against the initial concentrations of C_2H_2 . The measurements were performed at $T = 298$, 409 , and 438 K. The bimolecular rate constants derived from the slopes of the plots in Figure 1 are summarized in Table I.

The rate constants of reaction 1 were also measured in the LP/ST experiments. A typical example of the time profile of the absorption at 121.6 nm behind reflected shock waves is shown in Figure 2. In this figure, $t = 0$ is defined by the arrival of the reflected shock wave at the observation station and the photolysis

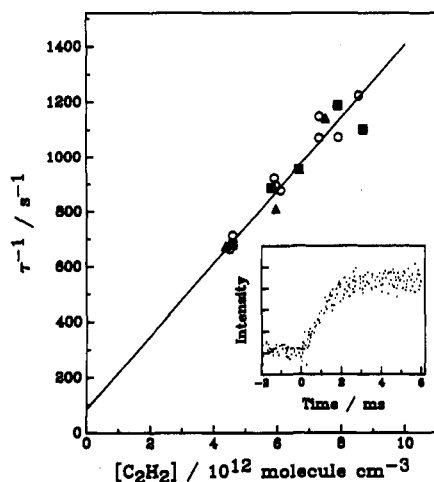


Figure 1. Pseudo-first-order rise rates of C_4H_2 ($m/z = 50$) vs $[C_2H_2]$ obtained in the LP/MS experiments. Total pressure was fixed at $p = 5$ Torr in He. Open circles, $T = 298$ K; closed triangles, $T = 409$ K; closed squares, $T = 438$ K. Insert shows an example of the time profile of C_4H_2 after the ArF laser photolysis of C_2H_2 ; $[C_2H_2] = 4.6 \times 10^{12}$ molecules cm^{-3} , $T = 298$ K.

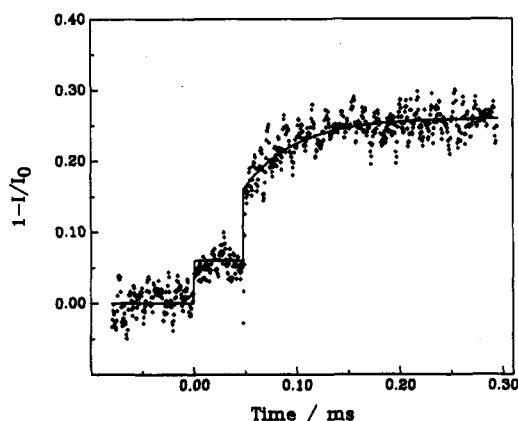


Figure 2. Example of the time profile of the absorption at 121.6 nm behind the reflected shock wave: $T = 1613$ K, $p = 1.4$ atm, and 20 ppm C_2H_2 in Ar. The ArF laser was fired at $t = 50$ μs .

laser was fired at $t = 50$ μs . The background absorption in the range of $t = 0$ – 50 μs is due to the absorption by shock-heated C_2H_2 .²⁶ This background absorption (i.e., the absorption without laser photolysis) was approximately constant behind the reflected shock wave under the present experimental conditions ($T = 1600$ – 2177 K and $P = 1.3$ – 2.2 atm), indicating that the H atom production by the thermal decomposition of C_2H_2 was negligible. This was also confirmed by the numerical simulation based on the reaction mechanism for the thermal decomposition of C_2H_2 proposed by Frank and Just.²⁶ At $T = 2000$ K and $P = 2.2$ atm, the H atoms produced by the thermal decomposition at $t = 300$ μs were estimated to be $[H] = 1.8 \times 10^{-4}[C_2H_2]$, which was much lower than the H atoms produced by laser photolysis ($[H] \approx 2 \times 10^{-3}[C_2H_2]$). Following instantaneous production of H atoms due to the ArF laser photolysis of C_2H_2 at $t = 50$ μs , the absorption intensity gradually increased to a steady-state level. The time profiles of H atoms after photolysis were fitted to a single-exponential function to determine the pseudo-first-order rate constants. The resulting bimolecular rate constants of reaction 1 at shock-tube temperatures are also included in Table I. It is clear from this table that the rate constants of reaction 1 are constant over the temperatures 298–2177 K. The rate constant of $k_1 = (1.5 \pm 0.3) \times 10^{-10}$ cm^3 molecule $^{-1}$ s $^{-1}$ was obtained by a simple average of all the values. The present high-temperature values of k_1 are larger than those of our previous report ($k_1 = (6.6 \pm 1.1) \times 10^{-11}$ cm^3 molecule $^{-1}$ s $^{-1}$ at $T = 1565$ – 2218 K).¹⁰ This is caused by inadequate procedures for the least-squares fit. It was found that the values of $[H]_\infty$ were incorrect in the previous

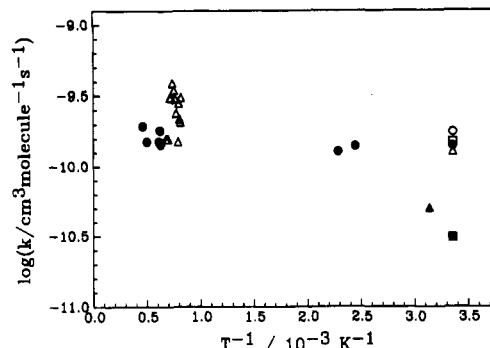


Figure 3. Arrhenius plot of the rate constant of the $C_2H + C_2H_2$ reaction. Closed circles, this work; open circles, Koshi et al. (ref 9); open triangles, Shin and Michael (ref 8); closed triangles, Lange and Wagner (ref 6); open squares, Stephens et al. (ref 7); closed squares, Laufer and Bass (ref 2).

analysis, and a plot of τ^{-1} against $[C_2H_2]$ had a non-zero intercept at $[C_2H_2] = 0$. Since the heterogeneous loss of the C_2H reactant in shock waves should be neglected, the value of τ^{-1} should be zero at $[C_2H_2] = 0$. In the present analysis of the shock-tube data, the rate constants were determined by the linear least-squares fit of the plots of τ^{-1} against $[C_2H_2]$ under the constraint of zero intercept.

The present rate constants of reaction 1 are compared with all literature values except the incorrect values of our earlier reports^{10,13} in Figure 3. It should be noted that the rate constant derived from the decay rates of C_2H by Stephens et al.⁷ is in good agreement with the results of the present measurements of the appearance rates of the products, H and C_4H_2 . The present results also agree well with the results of Shin and Michael⁸ and the results of the room-temperature measurements by the vacuum UV-LIF detection of H atom.⁹ The lower value of Laufer and Bass² ($k_1 = (3.1 \pm 0.2) \times 10^{-11}$ cm^3 molecule $^{-1}$ s $^{-1}$) was derived from the appearance rates of C_4H_2 . Stephens et al. have suggested the formation of a stable intermediate (such as an isomer of C_4H_2 or C_4H_3) in order to explain the discrepancy between their value and that of Laufer and Bass. The formation of C_4H_3 from the C_2H precursor in the thermal polymerization in the pyrolysis of C_2H_2 has also been suggested by some researchers.^{27,28} Since the decay rates of C_2H and the appearance rates of H atoms were identical, Shin and Michael⁸ concluded that the formation of the stable C_4H_3 radical was ruled out. The present results further confirm their conclusion.

3.2. Reactions with H_2 and D_2 . The rate constants of reactions 2 and 3 were determined in the LP/MS experiments by measuring the dependence of the yields of C_4H_2 formation on the partial pressures of H_2 or D_2 . It was found that the yield of C_4H_2 formation decreased by the addition of H_2 or D_2 . This decrease is apparently caused by reaction 2 or reaction 3. By integrating the usual kinetic equations for reactions 1 and 2, the following equation for the C_4H_2 yield is obtained:

$$\frac{k_2}{k_1}[H_2] = \left(\frac{[C_2H]_0}{[C_4H_2]_\infty} - 1 \right) [C_2H_2] \quad (5)$$

Here, $[C_2H]_0$ is the concentration of C_2H initially formed by the photolysis of C_2H_2 , and $[C_4H_2]_\infty$ is the concentration of C_4H_2 at $t = \infty$. The value of $[C_2H]_0/[C_4H_2]_\infty$ is simply equal to the ratio of the signal intensities of C_4H_2 at $t = \infty$ with and without the addition of H_2 , since it was already confirmed that all the C_2H radical initially formed by the photolysis of C_2H_2 was converted to C_4H_2 in the absence of H_2 .⁹ The quantities on the right-hand side of eq 5 are plotted in Figure 4 against the concentrations of H_2 at several temperatures. The slope of this plot is equal to the ratio of the rate constants, k_2/k_1 . The corresponding plots for reaction 3 are shown in Figure 5, and the resulting values of k_2/k_1 and k_3/k_1 are summarized in Table II.

There are four^{2,6,7,9} and two^{9,29} previous room-temperature measurements for reactions 2 and 3, respectively, including our recent measurements by vacuum UV-LIF detection of H atoms.⁹

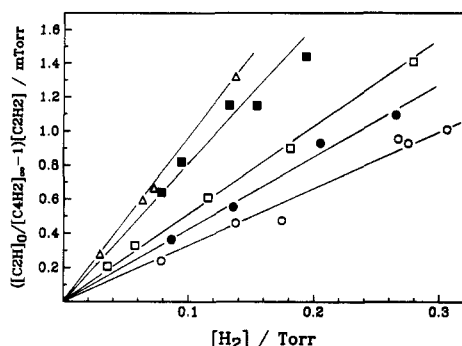


Figure 4. Plot of the RHS of eq 5 vs $[H_2]$. The slope of this plot is equal to the ratio k_2/k_1 . Open circles, $T = 298$ K; closed circles, $T = 349$ K; open squares, $T = 370$ K; closed squares, $T = 409$ K; open triangles, $T = 438$ K. Lines are the linear least-squares fit under the constraint of zero intercept.

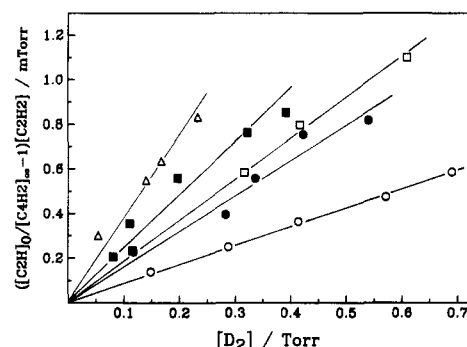


Figure 5. Plot of the RHS of eq 5 vs $[D_2]$. The slope of this plot is equal to the ratio k_3/k_1 . Open circles, $T = 298$ K; closed circles, $T = 349$ K; open squares, $T = 370$ K; closed squares, $T = 409$ K; open triangles, $T = 438$ K. Lines are the linear least-squares fit under the constraint of zero intercept.

TABLE II: Summary of the Ratio of the Rate Constants Obtained in the LP/MS Experiments^a

T/K	$(k_2/k_1)/10^{-3}$	$(k_3/k_1)/10^{-3}$
298	3.4 ± 0.2	0.87 ± 0.03
349	4.3 ± 0.2	1.7 ± 0.2
370	5.3 ± 0.6	1.9 ± 0.2
409	8.1 ± 0.6	2.6 ± 0.4
438	9.5 ± 0.2	4.2 ± 0.5

^a k_1 , k_2 , and k_3 are the rate constants for the $C_2H + C_2H_2$, $C_2H + H_2$, and $C_2H + D_2$ reactions, respectively. The errors are given to 2 standard deviations.

With a value of $k_1 = 1.5 \times 10^{-10} \text{ cm}^3 \text{ molecule}^{-1} \text{ s}^{-1}$, the present rate constants, k_2 and k_3 , are compared with previous literature values in Figure 6. In this figure, our previous values^{10,13} of k_2 at high temperatures are omitted, since the accuracy of these values are questionable as described below. The room-temperature rate constants derived from the vacuum UV-LIF experiments ($k_2 = (7.1 \pm 1.1) \times 10^{-13}$ and $k_3 = (2.0 \pm 0.3) \times 10^{-13} \text{ cm}^3 \text{ molecule}^{-1} \text{ s}^{-1}$)⁹ are higher than the LP/MS results ($k_2 = (5.1 \pm 2.0) \times 10^{-13}$ and $k_3 = (1.3 \pm 0.5) \times 10^{-13} \text{ cm}^3 \text{ molecule}^{-1} \text{ s}^{-1}$), but these values overlap one another within combined uncertainties. The errors (2 standard deviations) in the present values are estimated from the sum of the relative errors in the ratio of the rate constants (k_2/k_1 and k_3/k_1) and the absolute error in k_1 . The present results are also in agreement with the results of Stephens et al.⁷ and Landre et al.²⁹ within experimental error, but the rate constants of Laufer and Bass² and Lange and Wagner⁶ for reaction 2 are much lower than the present value, as is the case of reaction 1.

From the values in Table II, simple Arrhenius expressions for reactions 2 and 3 can be obtained by using the temperature-independent rate constant of reaction 1: $k_2 = (1.8 \pm 1.0) \times 10^{-11} \exp(-1090 \pm 299/T) \text{ cm}^3 \text{ molecule}^{-1} \text{ s}^{-1}$ and $k_3 = (1.4 \pm 0.8) \times 10^{-11} \exp(-1377 \pm 301/T) \text{ cm}^3 \text{ molecule}^{-1} \text{ s}^{-1}$. A TST calculation by Harding et al.³⁰ for reaction 1, with ab initio transition-state properties,

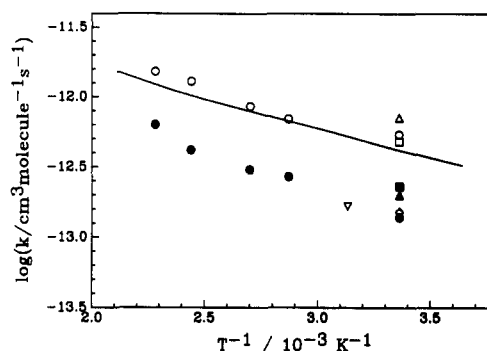


Figure 6. Arrhenius plots of the rate constants of the $C_2H_2 + H_2$ (open points) and the $C_2H_2 + D_2$ (closed points) reactions. \circ and \bullet , this work; Δ and \blacktriangle , Koshi et al. (ref 9); \square , Stephens et al. (ref 7); \blacksquare , Landre et al. (ref 27); \diamond , Laufer and Bass (ref 2); ∇ , Lange and Wagner (ref 6). The line is the result of the TST calculation using the POL-CI transition-state properties with the classical barrier height of 2 kcal/mol.

predicted highly non-Arrhenius behavior at high temperatures. Therefore, the above Arrhenius expressions are valid only in the temperature range 298–438 K.

Unsuccessful attempts have been made to determine the high-temperature rate constant of reaction 2 in the LP/ST experiments. Since the rate of reaction 1 is already very fast, a low concentration of C_2H_2 was required to observe the acceleration in H atom production by the addition of H_2 . However, enough signal intensity could not be obtained with such low concentrations of C_2H_2 . Our previous report¹⁰ on the rate constant of reaction 2 was based on the erroneous low value of k_1 . Reanalysis of the data indicated that the production of the H atom in the previous experiment was still dominated by reaction 1. Hence, the accuracy of our previous values is questionable.

In Figure 6, the present rate constants for reaction 2 are also compared with the results of a conventional TST calculation that uses the POL-CI transition state obtained by Harding et al. Since they estimated that the POL-CI classical barrier height of $V^* = 4.0$ kcal/mol was too high by 1.2–2 kcal/mol, the value of V^* was adjusted so that agreement with experimental values could be achieved. If Wigner tunneling corrections are included, good agreement is obtained with the barrier height of $V^* = 2$ kcal/mol. This TST calculation indicates that the tunnel effect is important at temperatures below 1000 K.

The ab initio calculations of Harding et al.³⁰ predicted a linear transition state that is located in the reactant region in the phase space. The H–H bond length in the POL-CI transition state is only 6% greater than in the unreacted H_2 molecule. In this case, one would expect little change in the activation energy between $C_2H + D_2$ and $C_2H + H_2$ reactions, since the zero-point energy correction might be similar for such loose transition states. The difference in rate constants would depend mainly on the pre-exponential factor that is dependent on average relative velocities and the vibrational and rotational partition functions. The ratio of the relative velocities for $C_2H + D_2/C_2H + H_2$ is equal to $2^{-1/2}$, and the ratio of the rotational partition functions with the POL-CI transition-state geometry is equal to 0.73. Thus, the isotope effect, when expressed as the ratio of rate constants k_3/k_2 , is expected to be 0.52 if the difference in the vibrational partition functions and the tunnel effect are neglected. According to Wigner's theory, the isotope effect for the tunneling is determined by the imaginary normal-mode vibrational frequency associated with the reaction coordinate. Since no ab initio calculation on the $C_2H + D_2$ reaction has been reported, we use the result of the MP2/6-31G** calculation.⁹ The transition-state geometry calculated at the MP2/6-31G** level also has linear configuration and is similar to the POL-CI transition state, but the classical barrier height is 4.76 kcal/mol. The vibrational frequencies for the transition state at the MP2/6-31G** level are 81.9 (2), 549 (2), 822 (2), 2526, 3524, 3616, and 774i cm^{-1} for the $C_2H + H_2$ reaction and 73 (2), 390(2), 821 (2), 2459, 2566, 3615, and 557i cm^{-1} for the $C_2H + D_2$ reaction. The D/H ratio of the isotope effect for the Wigner tunneling correction is equal to 0.74 at 298 K and 0.84

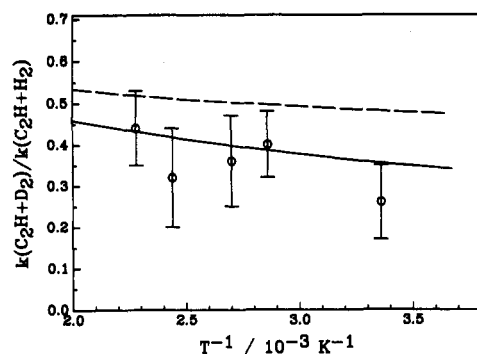


Figure 7. Temperature dependence of the ratio of the rate constant for the $C_2H + D_2/H_2$ reactions. Lines are the results of the TST calculation using the MP2/6-31G** transition-state properties: Solid curve, with the Wigner tunneling correction; broken curve, without tunneling correction. Open circles with error bars are the results of the present experiments.

at 438 K. Thus, the ratio k_3/k_2 is estimated to be 0.38 at 298 K and 0.45 at 438 K by neglecting the difference in the ratio of the vibrational partition function. This value is close to the present result of $k_3/k_2 = 0.26 \pm 0.09$ at 298 K and 0.44 ± 0.14 at 438 K. For a more precise evaluation of the isotope effects, the values of k_3/k_2 were calculated on the basis of conventional TST theory. It should be noted that the ratio k_3/k_2 is independent of V^\ddagger and depends on the normal-mode vibrational frequencies and the moment of inertia of the transition state. The results are compared with the experimental results in Figure 7. The ratio k_3/k_2 is around 0.5 without the tunneling correction, as expected from the above discussion, and inclusion of the Wigner tunneling correction gives better agreement with the experimental results.

4. Conclusions

The main conclusions obtained in this work are summarized as follows:

(1) The rate constants for the $C_2H + C_2H_2 \rightarrow C_2H_2 + H$ reaction were determined by using two different experimental techniques: LP/MS at $T = 298\text{--}438$ K and LP/ST at $T = 1600\text{--}2200$ K. No temperature dependence was found for this reaction, and the rate constants obtained in this work were in good agreement with the most recent results of Shin and Michael⁶ and with the room-temperature rate constant of Stephens et al.⁷ derived from the decay rates of the reactants.

(2) The temperature dependence of the rate constants for the $C_2H + H_2$ and $C_2H + D_2$ reactions was measured for the first time at $T = 298\text{--}438$ K by using a LP/MS technique. The present results agree well with the results of a conventional TST calculation coupled with the ab initio transition-state properties. The importance of the tunneling effect on these reactions is confirmed.

Registry No. C_2H , 2122-48-7; C_2H_2 , 74-86-2; H_2 , 1333-74-0; D_2 , 7782-39-0.

References and Notes

- (1) Kern, R. D.; Xie, K. *Prog. Energy Combust. Sci.* **1991**, *17*, 191.
- (2) Laufer, A. H.; Bass, A. M. *J. Phys. Chem.* **1979**, *83*, 310.
- (3) Renlund, A. M.; Shokoohi, F.; Reisler, H.; Wittig, C. *Chem. Phys. Lett.* **1981**, *84*, 293.
- (4) Renlund, A. M.; Shokoohi, F.; Reisler, H.; Wittig, C. *J. Phys. Chem.* **1982**, *86*, 4165.
- (5) Shokoohi, F.; Watson, T. A.; Reisler, H.; Kong, F.; Renlund, A. M.; Wittig, C. *J. Phys. Chem.* **1986**, *90*, 5695.
- (6) Lange, W.; Wagner, H. G. *Ber. Bunsen-Ges. Phys. Chem.* **1975**, *79*, 165.
- (7) Stephens, J. W.; Hall, J. L.; Solka, H.; Yan, W. B.; Curl, R. F.; Glass, G. P. *J. Phys. Chem.* **1987**, *91*, 5740.
- (8) Shin, K. S.; Michael, J. V. *J. Phys. Chem.* **1981**, *95*, 5864.
- (9) Koshi, M.; Nishida, N.; Matsui, H. *J. Phys. Chem.* **1992**, *96*, 5875.
- (10) Fukuda, K.; Koshi, M.; Yamasaki, K.; Matsui, H. *Proc. 18th Int. Symp. Shock Waves*, in press.
- (11) Koshi, M.; Miyoshi, A.; Matsui, H. *Chem. Phys. Lett.* **1991**, *184*, 442.
- (12) Koshi, M.; Miyoshi, A.; Matsui, H. *J. Phys. Chem.* **1991**, *95*, 9869.
- (13) Koshi, M.; Fukuda, K.; Matsui, H. *Prepr. Pap.-Am. Chem. Soc., Div. Fuel Sci.* **1991**, *36*, 1392.
- (14) Koshi, M.; Yoshimura, M.; Fukuda, K.; Matsui, H.; Saito, K.; Watanabe, M.; Imamura, A.; Chen, C. *J. Chem. Phys.* **1990**, *93*, 8703.
- (15) Yoshimura, M.; Koshi, M.; Matsui, H.; Kamiya, K.; Umeyama, H. *Chem. Phys. Lett.* **1992**, *189*, 199.
- (16) Seki, K.; Nakashima, N.; Nishi, N.; Kinoshita, M. *J. Chem. Phys.* **1986**, *85*, 274.
- (17) Okabe, H. *J. Chem. Phys.* **1975**, *62*, 2782.
- (18) Okabe, H.; Cody, R. J.; Allen, E., Jr. *Chem. Phys.* **1985**, *93*, 67.
- (19) Wodtke, A. M.; Lee, Y. T. *J. Phys. Chem.* **1985**, *89*, 4744.
- (20) Goodwin, P. M.; Cool, T. A. *J. Chem. Phys.* **1988**, *89*, 6600.
- (21) Laufer, A. H. *J. Phys. Chem.* **1981**, *85*, 3823.
- (22) Laufer, A. H.; Lechleider, R. J. *J. Phys. Chem.* **1984**, *88*, 66.
- (23) Satyapad, S.; Bersohn, R. *J. Phys. Chem.* **1991**, *95*, 8004.
- (24) Fahr, A.; Laufer, A. H. *J. Phys. Chem.* **1986**, *90*, 5064.
- (25) Michael, J. V.; Wagner, A. F. *J. Phys. Chem.* **1990**, *94*, 2094.
- (26) Frank, P.; Just, Th. *Combust. Flame* **1980**, *38*, 231.
- (27) Back, M. H. *Can. J. Chem.* **1971**, *49*, 2199.
- (28) Duran, R. P.; Amorebieta, V. T.; Colussi, A. J. *J. Phys. Chem.* **1990**, *92*, 636.
- (29) Landre, D. R.; Unfried, K. G.; Glass, G. P.; Curl, R. F. *J. Phys. Chem.* **1991**, *94*, 7759.
- (30) Harding, L. B.; Schatz, G. C.; Chiles, R. A. *J. Chem. Phys.* **1982**, *76*, 5172.